0026-895X/88/030377-11$02.00/0

MOLECULAR PHARMACOLOGY, 34:377-387



# Structure-Activity Relationship of Aldose Reductase Inhibitors Based on X-Ray Crystal Structures of Oxazolecarbamate Derivatives

TOSHIMASA ISHIDA, YASUKO IN, HIROFUMI OHISHI, DAISUKE YAMAMOTO, MASATOSHI INOUE, CHIAKI TANAKA, YOKO UENO, YOSHIROU OHMOMO, NANA KANDA, AKIRA TANAKA, and TSUYOSHI TANIMOTO

*Osaka University of Pharmaceutical Sciences, 2-10-65 Kawai, Matsubara, Osaka 580 (T.I., Y.I., H.O., D.Y., M.I., C.T., Y.U., Y.O.), and National Institute of Hygienic Sciences, 1-18-1 Kami-Yoga, Setagaya-ku, Tokyo 158, Japan (N.K., A.T., T.T.)*

Received February 24, 1988; Accepted June 2, 1988

**SUMMARY**

In order to elucidate the key atoms and/or stereostructures necessary for the inhibitory emergence of aldose reductase, crystal structure determinations were carried out for 11 oxazolecarbamate analogues, which have similar chemical and physicochemical properties but different inhibitory activities. The molecular conformations, revealed by X-ray analyses, were also ascertained to be energetically stable from theoretical conformational energy calculations. A surprising degree of conformational similarity was observed for the potent inhibitors. The analyses of the quantitative structure—activity relationships showed that the molecular conformation and the dipole moment, as well as the hydrophobicity at the oxazole C5-site, were important for high activity.

Aldose reductase (EC 1.1.1.21), one of the NADPH-dependent aldoketo reductases, is the first enzyme of the polyol pathway and catalyses the reduction of hexoses to their respective sugar alcohols. Sorbitol accumulates in the lens (1, 2), peripheral nerves (3, 4), and retina (5, 6) of diabetic humans and animals. Elevated sorbitol levels result in a loss of osmotic integrity and subsequent cellular damage (7, 8), which are linked to development of some complications of diabetes such as cataracts, neuropathy, retinopathy, and nephropathy (9, 10). Because excessive sorbitol is produced from glucose by aldose reductase, increased importance has been placed on the development of potent aldose reductase inhibitors, which are viewed as a means to reduce chronic diabetic complications. Several compounds with different chemical structures, such as sorbinil (11), ONO-2235 (12), and tolrestat (13), were suspected to be therapeutic. Recently, benzyl 4-isopropyl-5-phenyl-2-oxazolecarbamate was found to be a potent aldose reductase inhibitor (14, 15).

In order to develop more potent inhibitors, it is important to elucidate the key atoms, and their spatial orientations, necessary for activity emergence (16). A possible methodology is to compare the stereostructures in a series of compounds with similar chemical and physicochemical properties but different pharmaceutical activities. Because the inhibition for aldose reductase in rabbit lens has already been elucidated for the 2-oxazolecarbamate analogues (14, 15) listed in Table 1, we have undertaken in this study the X-ray single crystal structural analyses of these compounds (except **4**) and have considered the structure—activity relationship.

## Materials and Methods

All compounds have been chemically synthesized (14, 15).

**X-ray analyses.** Various attempts to crystallize compound **4** were unsuccessful. The crystallographic data for the other compounds are given in Table 2. Unit-cell dimensions and diffraction intensities were measured in a similar manner with graphite-monochromated Cu K$\alpha$ radiation ($\lambda$ = 1.5418 Å) on a Rigaku AFC-5 computer-controlled diffractometer. The unit-cell parameters were determined by a least squares fit to $2\theta$ angles for 20 to 25 reflections ($30° < 2\theta < 60°$). The crystal density was measured by the flotation method using a $CCl_4/C_6H_6$ mixture. The collected intensity data with $\omega - 2\theta$ scan technique were corrected for Lorentz and polarization effects but not for absorption. Non-hydrogen atom positions were located by a combination of direct method (17) and Fourier syntheses and refined by a block-diagonal least squares method using anisotropic thermal parameters. The positions of the geometrically ideal hydrogen atoms were calculated, which were verified on respective difference Fourier maps, except for compounds **9** and **12**, and included in subsequent refinements (only in the calculations of structure amplitudes for compounds **9** and **12**) with isotropic temperature factors. The function minimized was $\sum w(|F_o| - |F_c|)^2$, where $|F_o|$ and $|F_c|$ are the observed and calculated structure amplitudes, respectively. The weighting scheme used for the refinement was the following: $w = a$ for $F_o = 0.0$, and $w = 1.0/[\sigma(F_o)^2 + b|F_o| + c|F_o|^2]$ for $F_o > 0.0$, where $\sigma(F_o)^2$ is the standard deviation of the intensity based on counting statistics. The values of $a$, $b$, and $c$

**ABBREVIATIONS:** MSA, molecular surface area; CDV, conformational difference volume; D, debye; QSAR, quantitative structure-activity relationship.

TABLE 1

**Chemical structures used for study and their inhibitory activities, as well as atomic numbering scheme**

| Compound | R′ | K″ | $IC_{50}$ |
|---|---|---|---|
| | | 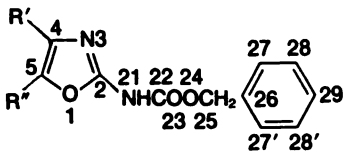 | μM |
| 1 | 42, 43, 41 $(CH_3)_2CH$ | 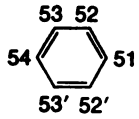 | 0.35 |
| 2 | $CH_3CH_2$ |  | 0.84 |
| 3 | $CH_3$ |  | 2.45 |
| 4 | $(CH_3)_3C$ |  | 12.9 |
| 5 | H |  | 15.6 |
| 6 | H | 52, 53, 54, 51 $(CH_3)_3C$ | 89.5 |
| 7 | $CH_3$ | $CH_3$ | 418 |
| 9 | H | $CH_3$ | 770 |
| 8 | 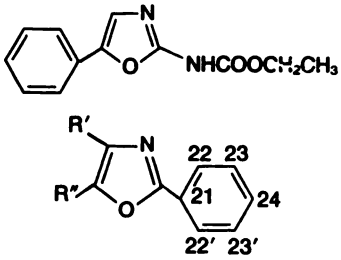 | | >500 |
| 10 | 41 $CH_3$ | 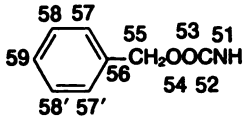 | 4010 |
| 11 | 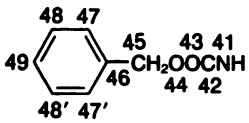 | H | ∞ |
| 12 | 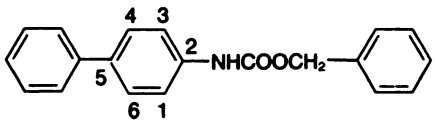 | | ∞ |

in the final refinement are also listed in Table 2, as well as the discrepancy indices, $R = (\sum ||F_o| - |F_c||/\sum |F_o|)$ and $R_w = [\sum w(|F_o| - |F_c|)^2/\sum w|F_o|^2]^{1/2}$, and goodness of fit, $S = [\sum w(|F_o| - |F_c|)^2/(M - N)]^{1/2}$, where $M$ and $N$ are the numbers of reflections used for refinement and atomic variables, respectively. For all crystallographic computations, the UNICs programs (18) were used, and the atomic scattering factors were cited from *International Tables for X-ray Crystallography* (19). The crystallographic details will be published elsewhere. Bond lengths and angles are given in Table 3. The atomic numbering used for all compounds is shown in Table 1.

**Conformational energy calculation.** The energy for conformational analysis was calculated by the molecular mechanics method

TABLE 2

**Summary of crystallographic data and structure refinement procedures**

| | 1 | 2 | 3 | 5 | 6 | 7 | 8 | 9 | 10 | 11 | 12 |
|---|---|---|---|---|---|---|---|---|---|---|---|
| Solvent for crystallization | Ethanol/ethylacetate | Benzene/*n*-hexane | Chloroform/*n*-exane | Chloroform/*n*-exane | Methanol/water | Methanol/water | Chloroform/*n*-exane | Methanol/water | Methanol/water | Methanol/water | Methanol/water |
| Crystal system | Tricli | Monocli | Monocli | Monocli | Monocli | Tricli | Orthorhom | Monocli | Tricli | Monocli | Orthorhom |
| Space group | $P\bar{1}$ | $P2_1/n$ | $P2_1/n$ | $P2_1/c$ | $C2/c$ | $P\bar{1}$ | $Pbcn$ | $P2_1/c$ | $P\bar{1}$ | $P2_1/a$ | $Pca2_1$ |
| Cell constant | | | | | | | | | | | |
| $a$, Å | 19.469 (7) | 9.131 (7) | 9.210 (7) | 6.928 (1) | 19.38 (2) | 11.086 (4) | 26.44 (1) | 4.663 (6) | 14.99 (5) | 12.017 (2) | 10.045 (2) |
| $b$, Å | 11.270 (3) | 18.81 (1) | 8.785 (6) | 17.255 (6) | 6.458 (4) | 8.544 (6) | 12.206 (8) | 10.48 (2) | 9.16 (4) | 9.745 (2) | 5.113 (1) |
| $c$, Å | 8.667 (3) | 9.680 (8) | 19.800 (9) | 25.406 (9) | 26.22 (3) | 7.406 (4) | 7.206 (4) | 23.28 (6) | 6.00 (2) | 13.923 (3) | 30.78 (1) |
| $\alpha$, deg | 95.48 (3) | 90 | 90 | 90 | 90 | 110.51 (4) | 90 | 90 | 107.8 (3) | 90 | 90 |
| $\beta$ | 99.61 (3) | 101.07 (3) | 99.60 (3) | 92.90 (4) | 109.81 (9) | 103.49 (3) | 90 | 90.9 (1) | 92.6 (5) | 113.65 (1) | 90 |
| $\gamma$ | 104.96 (3) | 90 | 90 | 90 | 90 | 94.35 (4) | 90 | 90 | 96.2 (4) | 90 | 90 |
| Volume, Å$^3$ | 1791 (1) | 1631 (2) | 1580 (2) | 3033 (2) | 3087 (5) | 929.2 (7) | 2326 (2) | 1137 (4) | 776 (5) | 1493.6 (5) | 1581.0 (8) |
| $Z$ | 4 | 4 | 4 | 8 | 8 | 2 | 8 | 4 | 2 | 4 | 4 |
| Formula/asymetric unit | 2 ($C_{20}H_{20}N_2O_3$) | $C_{19}H_{18}N_2O_3$ | $C_{18}H_{16}N_2O_3$ | 2($C_{17}H_{14}N_2O_3$) | $C_{18}H_{18}N_2O_3$ | $C_{13}H_{14}N_2O_3$ | $C_{12}H_{12}N_2O_3$ | $C_{12}H_{12}N_2O_3$ | $C_{16}H_{16}N_2O_3$ | $C_{17}H_{14}N_2O_3$ | $C_{20}H_{17}NO_2$ |
| $Dm$, g·cm$^{-3}$ | 1.266 (3) | 1.310 (3) | 1.299 (3) | 1.270 (2) | 1.201 (5) | 1.299 (2) | 1.321 (4) | 1.329 (5) | 1.319 (4) | 1.318 (6) | 1.280 (4) |
| $Dx$, g·cm$^{-3}$ | 1.247 | 1.313 | 1.296 | 1.289 | 1.180 | 1.300 | 1.326 | 1.357 | 1.319 | 1.309 | 1.274 |
| $\mu$(Cu K$\alpha$), cm$^{-1}$ | 5.93 | 6.92 | 7.72 | 6.99 | 6.44 | 7.36 | 7.66 | 7.84 | 7.05 | 7.10 | 6.19 |
| $F$(0 0 0) | 712 | 680 | 648 | 1232 | 1168 | 260 | 976 | 488 | 324 | 616 | 640 |
| Scan speed (in 2$\theta$), deg·min$^{-1}$ | 3 | 3 | 4 | 3 | 4 | 4 | 2 | 3 | 2 | 3 | 2 |
| Scan width in $A$ + $B$ tan $\theta$ | | | | | | | | | | | |
| $A$, deg | 0.80 | 1.10 | 1.00 | 1.10 | 1.00 | 1.00 | 1.00 | 1.50 | 1.90 | 1.20 | 1.40 |
| $B$, deg | 0.15 | 0.15 | 0.15 | 0.15 | 0.15 | 0.15 | 0.15 | 0.15 | 0.15 | 0.15 | 0.15 |
| No. of obsd. reflection | 6126 | 2772 | 2685 | 5168 | 2619 | 2132 | 1999 | 1956 | 2304 | 2548 | 1363 |
| No. used for refinement | 6126 | 2540 | 2192 | 3366 | 2619 | 2132 | 1668 | 1560 | 2304 | 2548 | 855 |
| ($I \geq n\sigma$ (I)) | 0 | 2 | 2 | 3 | 0 | 0 | 2 | 3 | 0 | 0 | 2 |
| Coefficient used in refinement | | | | | | | | | | | |
| $a$ | 1.110 | 0.0 | 0.0 | 0.0 | 0.193 | 4.731 | 0.0 | 0.0 | 0.384 | 1.988 | 0.0 |
| $b$ | −0.623 | −0.170 | −0.380 | −0.294 | −0.195 | −0.076 | −5.006 | 0.397 | −0.044 | −0.433 | 0.380 |
| $c$ | 0.032 | 0.013 | 0.022 | 0.022 | 0.010 | 0.010 | 0.224 | 0.006 | 0.005 | 0.026 | −0.003 |
| $R$ | 0.075 | 0.086 | 0.077 | 0.096 | 0.082 | 0.081 | 0.104 | 0.141 | 0.105 | 0.081 | 0.123 |
| $R_w$ | 0.082 | 0.127 | 0.074 | 0.152 | 0.097 | 0.141 | 0.086 | 0.201 | 0.095 | 0.107 | 0.071 |
| $S$ | 2.644 | 3.429 | 2.210 | 2.091 | 1.363 | 2.581 | 3.261 | 0.930 | 1.367 | 2.125 | 1.121 |
| $N$ | 612 | 290 | 273 | 510 | 254 | 220 | 203 | 155 | 273 | 248 | 209 |

TABLE 3

**Bond lengths and angles with estimated standard deviations in parentheses**

| | 1a | 1b | 2 | 3 | 5a | 5b | 6 | 7 | 8 | 9 | 10 | 11 | 12 |
|---|---|---|---|---|---|---|---|---|---|---|---|---|---|
| Length (Å) | | | | | | | | | | | | | |
| 1–2 | 1.338 (3) | 1.347 (3) | 1.335 (4) | 1.335 (3) | 1.343 (6) | 1.351 (6) | 1.330 (3) | 1.300 (5) | 1.359 (4) | 1.333 (8) | 1.354 (5) | 1.359 (4) | 1.39 (3) |
| 1–5 | 1.397 (3) | 1.403 (3) | 1.390 (4) | 1.408 (3) | 1.395 (6) | 1.407 (7) | 1.407 (7) | 1.411 (5) | 1.406 (4) | 1.398 (9) | 1.383 (5) | 1.377 (5) | |
| 1–6 | | | | | | | | | | | | | 1.43 (3) |
| 2–3 | 1.297 (3) | 1.287 (3) | 1.291 (5) | 1.289 (3) | 1.268 (7) | 1.275 (7) | 1.286 (3) | 1.333 (4) | 1.294 (4) | 1.281 (9) | 1.299 (5) | 1.284 (4) | 1.41 (2) |
| 2–21 | 1.364 (3) | 1.374 (3) | 1.370 (4) | 1.366 (3) | 1.367 (7) | 1.365 (7) | 1.370 (3) | 1.365 (5) | 1.362 (4) | 1.380 (9) | 1.454 (6) | 1.450 (5) | 1.42 (2) |
| 3–4 | 1.410 (3) | 1.399 (3) | 1.414 (5) | 1.410 (3) | 1.387 (7) | 1.402 (7) | 1.407 (4) | 1.399 (5) | 1.392 (4) | 1.39 (1) | 1.384 (5) | 1.378 (4) | 1.38 (3) |
| 4–5 | 1.345 (4) | 1.343 (8) | 1.341 (6) | 1.338 (4) | 1.354 (7) | 1.338 (8) | 1.318 (4) | 1.343 (5) | 1.341 (4) | 1.33 (1) | 1.324 (6) | 1.343 (5) | 1.34 (3) |
| 4–41 | 1.496 (4) | 1.501 (4) | 1.616 (7) | 1.491 (4) | | | | 1.481 (6) | | | 1.489 (6) | 1.393 (4) | |
| 5–6 | | | | | | | | | | | | | 1.39 (3) |
| 5–51 | 1.458 (4) | 1.456 (3) | 1.456 (5) | 1.460 (4) | 1.446 (8) | 1.457 (8) | 1.492 (4) | 1.481 (6) | 1.449 (4) | 1.48 (1) | 1.386 (5) | | 1.53 (3) |
| 21–22 | 1.379 (4) | 1.380 (3) | 1.377 (4) | 1.375 (4) | 1.355 (7) | 1.348 (7) | 1.377 (3) | 1.367 (5) | 1.351 (5) | 1.360 (9) | 1.381 (6) | 1.404 (5) | 1.30 (2) |
| 21–21′ | | | | | | | | | | | 1.388 (6) | 1.376 (5) | |
| 22–23 | 1.192 (4) | 1.192 (3) | 1.201 (4) | 1.194 (4) | 1.185 (7) | 1.209 (7) | 1.186 (3) | 1.189 (5) | 1.209 (4) | 1.205 (9) | 1.399 (7) | 1.397 (7) | 1.24 (2) |
| 22′–23′ | | | | | | | | | | | 1.377 (7) | 1.403 (6) | |
| 22–24 | 1.331 (3) | 1.337 (3) | 1.343 (4) | 1.338 (3) | 1.359 (7) | 1.335 (7) | 1.337 (3) | 1.346 (5) | 1.343 (4) | 1.327 (8) | | | 1.36 (2) |
| 23–24 | | | | | | | | | | | 1.374 (8) | 1.391 (7) | |
| 23′–24 | | | | | | | | | | | 1.357 (8) | 1.350 (6) | |
| 24–25 | 1.459 (4) | 1.455 (4) | 1.465 (4) | 1.459 (3) | 1.448 (8) | 1.473 (8) | 1.448 (4) | 1.464 (5) | 1.443 (5) | 1.45 (1) | | | 1.45 (2) |
| 25–26 | 1.500 (4) | 1.509 (4) | 1.502 (5) | 1.482 (4) | 1.500 (9) | 1.498 (9) | 1.496 (4) | 1.508 (6) | 1.474 (6) | 1.50 (1) | | | 1.50 (3) |
| 26–27 | 1.382 (4) | 1.383 (4) | 1.388 (5) | 1.391 (4) | 1.369 (9) | 1.37 (1) | 1.374 (4) | 1.376 (6) | | 1.37 (1) | | | 1.38 (3) |
| 26–27′ | 1.375 (4) | 1.375 (4) | 1.383 (5) | 1.379 (4) | 1.375 (9) | 1.41 (1) | 1.381 (4) | 1.386 (6) | | 1.40 (1) | | | 1.35 (3) |
| 27–28 | 1.394 (5) | 1.373 (5) | 1.402 (5) | 1.365 (4) | 1.39 (1) | 1.39 (1) | 1.393 (5) | 1.390 (6) | | 1.41 (1) | | | 1.41 (4) |
| 27′–28′ | 1.373 (5) | 1.404 (5) | 1.386 (6) | 1.412 (5) | 1.37 (1) | 1.37 (1) | 1.389 (5) | 1.376 (6) | | 1.40 (1) | | | 1.38 (3) |
| 28–29 | 1.365 (6) | 1.376 (5) | 1.374 (6) | 1.338 (6) | 1.39 (1) | 1.39 (1) | 1.373 (5) | 1.383 (7) | | 1.34 (1) | | | 1.41 (4) |
| 28′–29 | 1.356 (6) | 1.371 (5) | 1.361 (6) | 1.370 (6) | 1.39 (1) | 1.34 (1) | 1.370 (6) | 1.384 (7) | | 1.40 (1) | | | 1.36 (3) |
| 41–42 | 1.526 (5) | 1.536 (4) | 1.406 (8) | | | | | | | | | 1.347 (4) | |
| 41–43 | 1.531 (5) | 1.534 (4) | | | | | | | | | | | |
| 42–43 | | | | | | | | | | | | 1.204 (4) | |
| 42–44 | | | | | | | | | | | | 1.345 (4) | |
| 44–45 | | | | | | | | | | | | 1.455 (5) | |
| 45–46 | | | | | | | | | | | | 1.502 (5) | |
| 46–47 | | | | | | | | | | | | 1.370 (5) | |
| 46–47′ | | | | | | | | | | | | 1.376 (5) | |
| 47–48 | | | | | | | | | | | | 1.370 (7) | |
| 47′–48′ | | | | | | | | | | | | 1.434 (7) | |
| 48–49 | | | | | | | | | | | | 1.346 (7) | |
| 48′–49 | | | | | | | | | | | | 1.379 (8) | |
| 51–42 | 1.395 (4) | 1.388 (4) | 1.395 (5) | 1.385 (4) | 1.395 (9) | 1.387 (9) | 1.537 (5) | | 1.401 (4) | | 1.400 (5) | | 1.35 (3) |
| 51–52′ | 1.394 (5) | 1.402 (4) | 1.394 (6) | 1.385 (4) | 1.388 (9) | 1.392 (9) | | | 1.390 (4) | | | | 1.37 (3) |
| 51–53 | | | | | | | 1.533 (6) | | | | | | |
| 51–54 | | | | | | | 1.507 (6) | | | | | | |
| 52–53 | 1.387 (4) | 1.387 (4) | 1.373 (6) | 1.383 (5) | 1.39 (1) | 1.41 (1) | | | 1.393 (5) | | 1.203 (5) | | 1.45 (3) |
| 52′–53′ | 1.396 (5) | 1.382 (4) | 1.397 (7) | 1.383 (5) | 1.39 (1) | 1.35 (1) | | | 1.393 (5) | | | | 1.39 (3) |
| 52–54 | | | | | | | | | | | 1.319 (5) | | |
| 53–54 | 1.367 (5) | 1.382 (4) | 1.398 (6) | 1.383 (5) | 1.41 (1) | 1.35 (1) | | | 1.389 (5) | | | | 1.36 (3) |
| 53′–54 | 1.384 (5) | 1.383 (4) | 1.361 (7) | 1.366 (5) | 1.37 (1) | 1.39 (1) | | | 1.376 (5) | | | | 1.31 (3) |
| 54–55 | | | | | | | | | | | 1.468 (6) | | |
| 55–56 | | | | | | | | | | | 1.504 (7) | | |
| 46–47 | | | | | | | | | | | 1.378 (7) | | |
| 56–57′ | | | | | | | | | | | 1.381 (7) | | |
| 57–58 | | | | | | | | | | | 1.395 (8) | | |
| 57′–58′ | | | | | | | | | | | 1.397 (7) | | |
| 58–59 | | | | | | | | | | | 1.369 (8) | | |
| 58′–59 | | | | | | | | | | | 1.371 (8) | | |
| Angle (°) | | | | | | | | | | | | | |
| 5–1–2 | 104.8 (2) | 103.8 (2) | 104.6 (3) | 104.1 (2) | 104.3 (4) | 103.6 (4) | 103.9 (2) | 104.2 (3) | 104.1 (2) | 104.1 (5) | | 104.5 (3) | |
| 6–1–2 | | | | | | | | | | | | | 118 (2) |

| | | | | | | | | | | | | | |
|---|---|---|---|---|---|---|---|---|---|---|---|---|---|
| 1–2–3 | 114.8 (2) | 115.4 (2) | 115.2 (3) | 115.6 (2) | 115.6 (5) | 115.8 (5) | 115.4 (2) | 115.1 (3) | 114.3 (3) | 115.8 (6) | | 113.8 (3) | 119 (2) |
| 1–2–21 | 118.7 (2) | 118.9 (2) | 119.7 (3) | 119.6 (2) | 119.9 (5) | 119.7 (5) | 121.3 (2) | 124.7 (3) | 120.4 (3) | 119.9 (6) | | 116.7 (3) | 117 (2) |
| 3–2–21 | 126.5 (2) | 125.7 (2) | 125.1 (3) | 124.8 (2) | 124.3 (5) | 124.5 (5) | 123.3 (2) | 120.2 (3) | 125.3 (3) | 124.2 (6) | | 129.5 (3) | 117 (2) |
| 2–3–4 | 104.1 (2) | 104.1 (2) | 103.7 (3) | 103.9 (2) | 104.3 (5) | 103.8 (5) | 103.7 (2) | 104.2 (3) | 104.6 (3) | 103.0 (6) | | 104.7 (3) | 121 (2) |
| 3–4–5 | 109.2 (2) | 109.7 (2) | 108.9 (4) | 109.4 (2) | 110.0 (5) | 110.2 (5) | 109.7 (2) | 108.0 (3) | 110.2 (3) | 111.1 (7) | | 110.0 (3) | 121 (2) |
| 3–4–41 | 122.0 (2) | 121.8 (2) | 119.5 (4) | 120.0 (2) | | | | 116.7 (3) | | | | 119.2 (3) | |
| 5–4–41 | 128.7 (3) | 128.5 (2) | 130.5 (4) | 130.6 (3) | | | | 135.3 (4) | | | | 130.8 (3) | |
| 1–5–4 | 107.1 (2) | 107.1 (2) | 107.5 (3) | 107.1 (2) | 105.9 (4) | 106.6 (5) | 107.3 (2) | 108.5 (3) | 106.8 (3) | 105.9 (6) | | 106.9 (3) | |
| 4–5–6 | | | | | | | | | | | | | 119 (2) |
| 4–5–51 | 138.7 (3) | 136.5 (2) | 136.6 (4) | 137.7 (3) | 136.5 (5) | 136.3 (5) | 136.5 (3) | 129.1 (4) | 136.5 (3) | 137.1 (7) | | | 122 (2) |
| 1–5–51 | 114.2 (2) | 116.4 (2) | 115.8 (3) | 115.2 (2) | 117.5 (4) | 117.0 (5) | 116.2 (2) | 122.4 (3) | 116.6 (3) | 116.9 (6) | | | 119 (2) |
| 1–6–5 | | | | | | | | | | | | | 121 (2) |
| 2–21–22 | 123.9 (2) | 123.9 (2) | 123.7 (3) | 124.7 (2) | 128.8 (5) | 129.6 (5) | 126.3 (2) | 125.5 (3) | 127.3 (3) | 126.5 (6) | | 119.0 (3) | 125 (2) |
| 2–21–22′ | | | | | | | | | | | | 121.8 (3) | |
| 22–21–22′ | | | | | | | | | | | | 119.2 (3) | |
| 21–22–23 | 126.0 (3) | 126.1 (3) | 126.4 (3) | 126.2 (3) | 126.6 (5) | 127.2 (5) | 127.6 (2) | 127.6 (4) | 126.9 (3) | 126.2 (7) | | 119.6 (4) | 130 (2) |
| 21–22–24 | 108.8 (2) | 107.9 (2) | 108.2 (3) | 108.0 (2) | 107.0 (5) | 108.5 (5) | 105.9 (2) | 107.6 (3) | 107.8 (3) | 108.4 (6) | | | 110 (1) |
| 23–22–24 | 125.3 (3) | 126.0 (3) | 125.4 (3) | 125.7 (3) | 126.4 (5) | 124.2 (5) | 126.6 (2) | 124.8 (4) | 125.3 (3) | 125.4 (7) | | | 120 (2) |
| 21–22′–23′ | | | | | | | | | | | | 120.2 (3) | |
| 22–23–24 | | | | | | | | | | | | 120.2 (5) | |
| 22′–23′–24 | | | | | | | | | | | | 120.9 (4) | |
| 22–24–25 | 116.3 (2) | 115.5 (2) | 116.1 (3) | 115.8 (2) | 113.6 (5) | 116.2 (5) | 117.2 (2) | 116.2 (3) | 115.4 (3) | 115.0 (6) | | | 117 (1) |
| 23–24–23′ | | | | | | | | | | | | 120.0 (4) | |
| 24–25–26 | 110.9 (2) | 112.5 (2) | 110.4 (3) | 110.9 (2) | 106.8 (5) | 107.1 (5) | 105.6 (2) | 110.2 (3) | 108.2 (3) | 108.3 (6) | | | 104 (2) |
| 25–26–27 | 120.5 (3) | 118.4 (3) | 121.1 (3) | 119.7 (3) | 120.1 (6) | 119.9 (6) | 120.3 (3) | 120.6 (3) | | 122.7 (7) | | | 120 (2) |
| 25–26–27′ | 120.2 (3) | 122.0 (3) | 119.6 (3) | 121.8 (3) | 120.4 (6) | 120.4 (6) | 120.2 (3) | 120.3 (3) | | 117.1 (7) | | | 121 (2) |
| 27–26–27′ | 119.3 (3) | 119.5 (3) | 119.3 (3) | 118.4 (3) | 119.3 (6) | 119.7 (6) | 119.6 (3) | 119.1 (4) | | 120.2 (7) | | | 119 (2) |
| 26–27–28 | 118.9 (3) | 120.8 (3) | 120.1 (3) | 121.1 (3) | 120.5 (7) | 118.6 (7) | 120.2 (3) | 120.0 (4) | | 118.6 (7) | | | 119 (2) |
| 26–27′–28′ | 120.6 (3) | 119.9 (3) | 119.8 (4) | 119.8 (3) | 120.3 (6) | 119.5 (7) | 120.4 (3) | 121.4 (4) | | 119.3 (8) | | | 123 (2) |
| 27–28–29 | 120.9 (4) | 119.8 (3) | 119.5 (4) | 120.3 (4) | 120.2 (7) | 121.3 (7) | 119.6 (3) | 120.5 (4) | | 122.3 (8) | | | 121 (2) |
| 27′–28′–29 | 120.6 (4) | 119.4 (3) | 121.0 (4) | 118.9 (3) | 119.7 (7) | 121.5 (8) | 119.5 (4) | 119.5 (4) | | 119.9 (9) | | | 120 (2) |
| 28–28–28′ | 119.6 (4) | 120.6 (3) | 120.3 (4) | 121.5 (4) | 119.9 (8) | 119.3 (8) | 120.7 (4) | 119.6 (4) | | 119.6 (9) | | | 118 (2) |
| 4–41–42 | 111.0 (3) | 110.1 (2) | 103.4 (4) | | | | | | | | 122.4 (3) | | |
| 4–41–43 | 111.5 (3) | 111.1 (2) | | | | | | | | | | | |
| 42–41–43 | 111.3 (3) | 111.3 (2) | | | | | | | | | | | |
| 41–42–43 | | | | | | | | | | | 124.8 (3) | | |
| 41–42–44 | | | | | | | | | | | 110.2 (3) | | |
| 43–42–44 | | | | | | | | | | | 125.0 (3) | | |
| 42–44–45 | | | | | | | | | | | 117.2 (3) | | |
| 44–45–46 | | | | | | | | | | | 110.8 (3) | | |
| 45–46–47 | | | | | | | | | | | 120.5 (3) | | |
| 45–46–47′ | | | | | | | | | | | 119.4 (3) | | |
| 47–46–47′ | | | | | | | | | | | 120.1 (4) | | |
| 46–47–48 | | | | | | | | | | | 120.5 (4) | | |
| 46–47′–48′ | | | | | | | | | | | 118.9 (4) | | |
| 47–48–49 | | | | | | | | | | | 121.2 (5) | | |
| 47′–48′–49 | | | | | | | | | | | 118.8 (5) | | |
| 48–49–48′ | | | | | | | | | | | 120.5 (5) | | |
| 5–51–52 | 119.5 (3) | 121.1 (2) | 118.5 (3) | 120.6 (2) | 119.1 (5) | 119.1 (5) | 109.5 (3) | | 119.4 (3) | | | | 120 (2) |
| 5–51–52′ | 122.0 (3) | 120.2 (2) | 120.1 (3) | 120.5 (2) | 120.5 (5) | 121.9 (6) | | | 121.8 (3) | | | | 120 (2) |
| 52–51–52′ | 118.5 (5) | 118.8 (2) | 121.4 (3) | 118.9 (3) | 120.3 (6) | 119.0 (6) | | | 118.7 (3) | | | | 120 (2) |
| 5–51–53 | | | | | | | 109.7 (3) | | | | | | |
| 5–51–54 | | | | | | | 108.4 (3) | | | | | | |
| 52–51–53 | | | | | | | 108.2 (3) | | | | | | |
| 52–51–54 | | | | | | | 109.5 (3) | | | | | | |
| 53–51–54 | | | | | | | 111.5 (3) | | | | | | |
| 51–52–53 | 120.6 (3) | 120.9 (2) | 120.4 (4) | 120.1 (3) | 119.2 (6) | 119.8 (6) | | | 119.8 (3) | | | | 119 (2) |
| 51–52′–53′ | 119.6 (3) | 119.8 (2) | 120.0 (4) | 120.5 (3) | 119.8 (6) | 120.3 (7) | | | 120.3 (3) | | | | 120 (2) |
| 52–53–54 | 121.4 (3) | 120.1 (3) | 121.1 (4) | 120.6 (3) | 120.9 (7) | 119.8 (7) | | | 119.9 (3) | | | | 119 (2) |
| 52′–53′–54 | 121.5 (3) | 121.0 (3) | 121.3 (4) | 120.6 (6) | 120.9 (7) | 121.0 (8) | | | 120.0 (3) | | | | 121 (2) |
| 53–54–53′ | 118.5 (3) | 119.4 (3) | 118.5 (4) | 119.3 (3) | 119.5 (7) | 120.0 (8) | | | 120.5 (3) | | | | 121 (2) |

[CHEMLAB-II version (20)]. The energy functions included in the calculation were steric (Lennard-Jones potential), electrostatic (Coulombic), and torsional energies:

$$E_{steric} = \sum_i \sum_j (-A_{ij} r_{ij}^{-6} + B_{ij} r_{ij}^{-12}) \quad (1)$$

$$E_{elec} = \sum_i \sum_j 332.0 \cdot Q_i \cdot Q_j \cdot r_{ij} \epsilon^{-1} \quad (2)$$

$$E_{tor} = A[B + C \cos^M(N\theta - \phi)] + D[1 - \cos(E\theta - \psi)] \quad (3)$$

where $r_{ij}$ in Eqs. 1 and 2 is the distance (in angstroms) between atoms $i$ and $j$. The atomic net charge on atom $i$ ($Q_i$) in Eq. 2 was calculated by the CNDO/2 method (21), and the dielectric constant ($\epsilon$) was taken as 4.0, close to the experimental values for biomolecules in polar media. The $A$, $B$, $C$, $D$, $E$, $M$, $N$, $\theta$, $\phi$, and $\psi$ in Eq. 3 are constants associated with a particular type of bond (22). All calculations of Eqs. 1–3 were performed with the supplied data set (20). The notation of variable torsion angles is shown in Table 4. Among the torsion angles, $\omega_3$(C2 — N21-C22-024) was set to 180° (*trans*) for all calculations, because the amide bond shows a strong preference for that value. In the conformational analysis, respective torsions were rotated simultaneously in 10° increments from 0° to 360° (for $\omega_1$ and $\omega_6$, 0° to 180°), where the starting, eclipsed conformation was 0°.

**Dipole moments.** The dipole moments ($\mu_x$, $\mu_y$, and $\mu_z$) for each molecular conformation were calculated by the CNDO/2 method by using the atomic coordinates obtained by the present X-ray analyses.

**$^1$H NMR measurements.** $^1$H NMR spectra were measured on a Varian XL-300 (300 MHz for proton) spectrometer equipped with the temperature-controlled accessory (accuracy to ±1°). Chemical shifts were measured with tetramethylsilane as internal standard. The sample concentrations were determined by dry weight and then adjusted to the desired values by dilution. Spectra were recorded at each temperature of 30°, 40°, 50°, 60°, and 70°.

**Structure—activity correlation analysis.** In developing the correlation equations, the QSAR program in the CHEMLAB-II system (20) was used. We also considered the correlation of the conformational difference with the activity, using a molecular shape analysis method developed by Hopfinger (23); the molecular conformations of respective compounds were expressed by two values, MSA and CDV. MSA (in Å$^3$) was calculated using the van der Waals radii accepted for respective atoms. CDV (in Å$^3$) represents the difference van der Waals volume from a reference compound, **1a**, for which the common overlap volume was set to the oxazole ring and was calculated using a numerical integration method developed by Pearlstein (24).

## Results and Discussion

### Molecular Dimensions and Conformations

Although some bond lengths and angles for the same chemical group differ slightly from one to another, the listed values within their estimated standard deviations all seem to lie in the expected region (see Table 3). All the oxazole and benzene rings essentially form planar structures with slight fluctuations, less than 0.02Å. The amide groups also take the usual *trans*-conformation ($\Delta\omega_{max}$ = 14.8(3)° for **2**).

Stereoscopic drawings, projected onto the oxazole ring, of a molecular unit for each of the compounds (**1–3, 5–12**) are presented in Fig. 1. Because both compounds **1** and **5** contain two crystallographically independent molecules per asymmetric unit, the respective molecular conformations are designated **a** and **b**. The torsion angles defining the carbamate side chain with respect to the oxazole ring are listed in Table 4. A conformational characteristic observed in 5-phenyl-2-oxazolecarbamate derivatives (**1–3, 5,** and **8**) is the coplanar formation of the oxazole ring with the phenyl and amide planes, $\omega_1$ and $\omega_2$ torsion angles are all in the *trans*- and *cis*-regions, respectively. The *cis* preference of $\omega_2$ is also observed in compounds **6, 7, 9,** and **11**. This is obviously due to the resonance effect between respective aromatic planes; the average bond lengths of C5—C51 (1.455Å) and C2—N21 (1.368Å) are in the partial double-bonded region. When torsion angles $\omega_4$ and $\omega_5$ are compared

TABLE 4

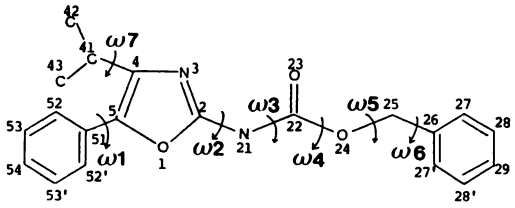


**Conformational torsion angles**

| | $\omega_1$[a] | $\omega_2$ | $\omega_3$ | $\omega_4$ | $\omega_5$ | $\omega_6$ |
|---|---|---|---|---|---|---|
| | | | degrees | | | |
| **1a** | 168.0 (3) | −7.1 (4) | 167.2 (2) | −176.8 (2) | 88.3 (3) | −94.6 (3) |
| **1b** | 143.7 (2) | −28.7 (3) | −177.3 (2) | −179.7 (2) | 81.1 (3) | −144.8 (3) |
| **2** | 171.6 (3) | −2.1 (5) | 165.2 (3) | −176.0 (3) | 87.6 (3) | −92.2 (4) |
| **3** | 175.0 (2)[b] | −5.6 (4 ( | 174.3 (2) | −175.2 (2) | 86.1 (3) | −96.8 (3)[c] |
| **5a** | 171.3 (5)[b] | −12.3 (8) | 179.4 (5) | 176.2 (5) | −179.1 (5) | −119.0 (6) |
| **5b** | −171.5 (5)[b] | 4.9 (9) | −176.3 (5) | −177.6 (5) | 179.0 (5) | −66.5 (8)[c] |
| **6** | | −25.4 (4) | −169.4 (2) | 179.5 (2) | −159.6 (2) | −98.5 (3) |
| **7** | | 160.6 (3) | −177.8 (3) | −172.1 (3) | 82.5 (4) | −130.0 (4) |
| **8** | −160.8 (3)[b] | −4.8 (5) | −178.6 (3) | 174.0 (3) | 178.2 (3) | |
| **9** | | −1 (1) | −177.5 (6) | −173.8 (6) | 172.1 (6) | −157.4 (7)[c] |
| **10**[d] | 174.3 (4)[b] | 102.1 (4) | −175.3 (3) | 178.8 (3) | 89.8 (4) | −97.7 (5) |
| **11**[d] | −174.6 (3)[b] | | 176.3 (3) | −176.7 (3) | −109.2 (3) | −102.4 (4)[c] |
| **12**[d] | | | −179 (2) | 177 (2) | 174 (1) | −120 (2) |

[a] $\omega_1$, 52′-51-5-1; $\omega_2$, 1-2-21-22; $\omega_3$, 2-21-22-24; $\omega_4$, 21-22-24-25; $\omega_5$, 22-24-25-26; $\omega_6$, 24-25-26-27.
[b] Torsion angles of 52-51-5-1 are listed.
[c] Torsion angles of 24-25-26-27′ are listed.
[d] Torsion angles corresponding to those in **1–9** are listed.

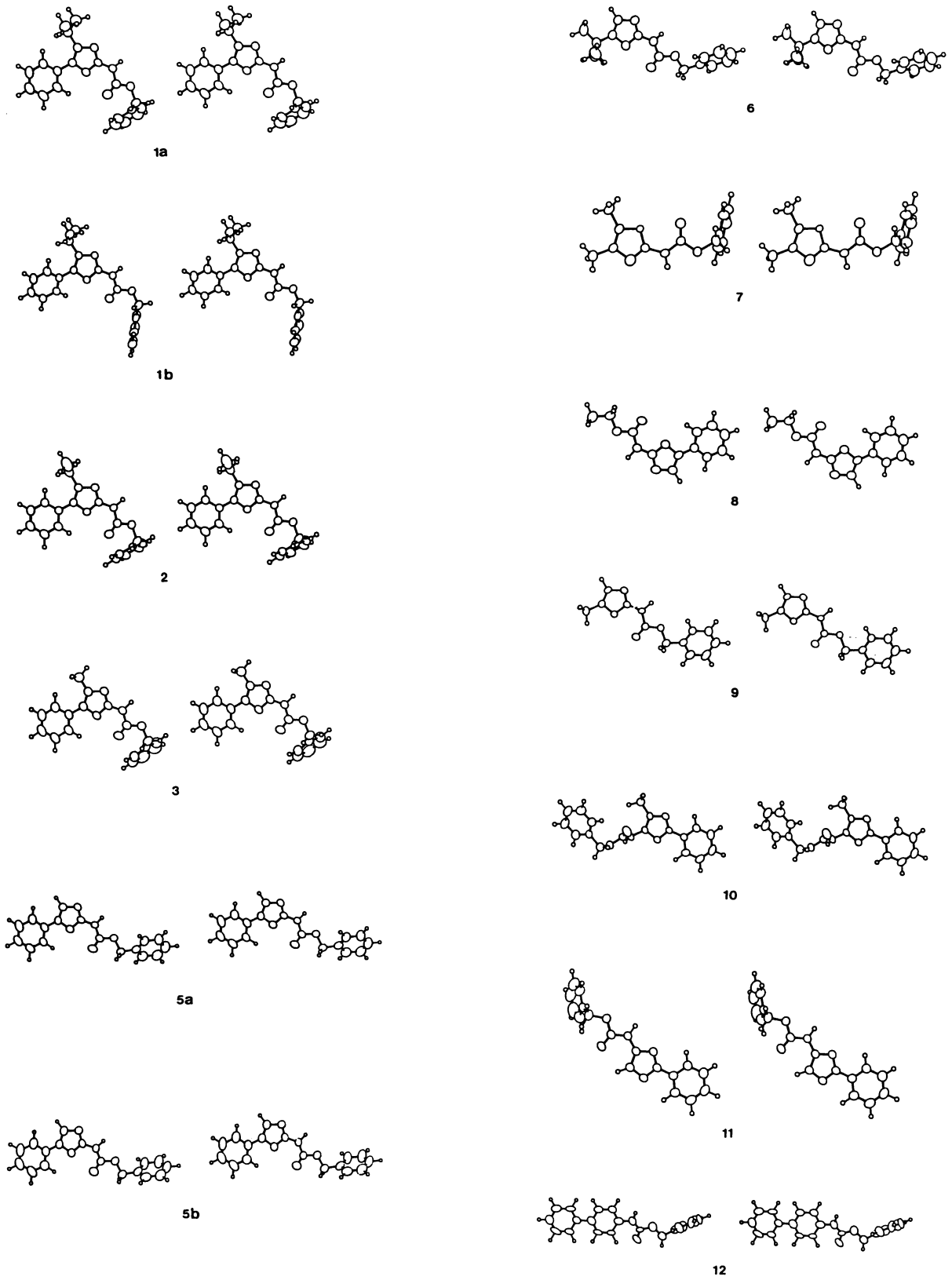


**Fig. 1.** Stereoscopic projections of **1-3** and **5-12** molecular conformations observed by X-ray analysis, projeted onto the oxazole ring.

with each other, it is also characteristic that $\omega_4$ is restricted to the *trans*-conformation, whereas $\omega_5$ rotates relatively freely. This would result from the difference between the C22-024 and 024-C25 bonding environments. The former bond (average value, 1.340Å) has a partial double-bond character; therefore, the *trans*-conformation is energetically stable. The latter one (average value 1.457Å) is in the normal, single-bonded region, allowing free rotation about this bond. Possible torsion angles

TABLE 5
**Hydrogen bonds and their patterns**

| | Hydrogen bonds | | Symmetry operation | Distance (Å) | Hydrogen-bonding pattern |
|---|---|---|---|---|---|
| | Donor at (x, y, z) | Acceptor at | | | |
| **1** | N21a | N3b | x, y, z | 2.999 (3) | NH . . . N dimer |
| | N21b | N3a | x, y, z | 2.979 (3) | |
| **2** | N21 | N3 | 1 − x, −y, 1 − z | 2.924 (4) | NH . . . N dimer |
| **3** | N21 | N3 | 2 − x, 1 − y, −z | 2.909 (3) | NH . . . N dimer |
| **5** | N21a | N3a | 2 − x, −y, 2 − z | 2.808 (7) | NH . . . N dimer |
| | N21b | N3b | 1− x, −y, 2 − z | 2.807 (7) | |
| **6** | N21 | N3 | −x, 1 − y, 1 − z | 2.838 (3) | NH . . . N dimer |
| **7** | N21 | 01 | −x, −y, −z | 2.935 (4) | NH . . . O dimer |
| **8** | N21 | N3 | 1 − x, −y, 1 − z | 2.830 (4) | NH . . . N dimer |
| **9** | N21 | N3 | 2 − x, 1 − y, 1 − z | 2.893 (9) | NH . . . N dimer |
| **10**[a] | N21 | N3 | x, y, z − 1 | 3.039 (5) | NH . . . N infinite chain |
| **11**[a] | N21 | 024 | 1:5 − x, y − 0.5, 1− z | 2.913 (4) | NH . . . O infinite chain |
| **12**[a] | N21 | 024 | x, 1 + y, z | 2.97 (2) | NH . . . O infinite chain |

[a] Numberings are different from the atomic parameters used for X-ray analyses for the sake of their comparisons with **1–9**.

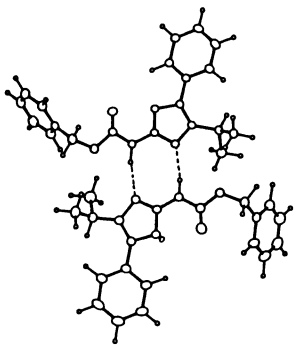

**Fig. 2.** N-H . . . N hydrogen-bonded dimer formation between compounds **1a** and **1b**.

of $\omega_6$ could be close to ±90° and ±150°. Among these, the alkyl side chain attached directly to the aromatic ring has preference for the torsion angle of ±90°. Compounds **1a**, **2**, **3**, **6**, **10**, and **11** also show this tendency.

**Characteristic hydrogen-bonding mode.** As summarized in Table 5, four kinds of hydrogen-bonding patterns are formed in the molecular packing of compounds **1–3** and **5–12**. Among these, the N12-H . . . N9 hydrogen-bonded dimer formation (type A), as exemplified in Fig. 2, is the most probable molecular packing mode for 2-oxazolecarbamate compounds in spite of the differences in crystal packing environments. Only compound **7** shows a different N12-H . . . O11 hydrogen-bonded dimer (type B). The predominance of type A over type B implies that the electron-acceptor ability of N3 is stronger than that of the O1 atom. It is interesting to note that the torsion angle $\omega_2$ is largely responsible for the hydrogen bonding modes of types A and B, as shown in the following scheme:

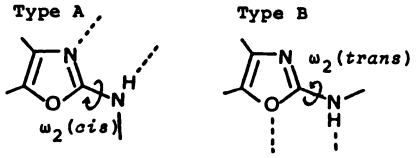


The hydrogen bonding modes observed in compounds **10–12** are basically different from those in **1–9**, because of the fundamental differences in their chemical structures.

These hydrogen-bonded dimer formations may also be formed in the solution state, with relatively high concentration. The downfield movements of N12-H proton chemical shifts ($\delta$) were observed in dimethyl sulfoxide-$d_6$ solutions of **1–9**, in proportion to the increase of the concentration (4–10 mM). Their shift values are in the range of 0.04–0.06 ppm, whereas those of **10–12** were not so significant (0.02–0.04 ppm). On the other hand, the temperature dependences of these NH protons at 4 mM concentration showed no hydrogen bonded aggregation, because the $d\delta/dT$ values (4.3 − 7.1 ppb/degree) are too large to consider as a defined conformation. This fact implies that each of **1–9** has the tendency to form a molecular aggregation, via hydrogen bonds, with the increase in the concentration, although they behave like a single molecule in dilute solution.

**Conformational analysis of oxazolecarbamate compounds and possible conformation of compound 4.** In order to estimate the conformational stabilities of oxazolecarbamate compounds as respective free molecules and, further, to consider the possible conformation of compound **4**, it is very important to ascertain whether the conformations observed by X-ray analyses correspond to the energetically stable ones. Contour energy maps for each of the two rotatable torsions, calculated by the molecular mechanics force field method using the atomic coordinates of **5a**, are shown in Fig. 3. The *filled circles* show the conformations observed by X-ray analyses. As seen in Fig. 3a, the low energy region for the ($\omega_1$, $\omega_2$) map has a relatively large rotational freedom. The *cis*-conformation of $\omega_2$ allows larger freedom than the *trans*-conformation. The *cis* preference of $\omega_2$ in the X-ray analyses does not conflict with this result. The X-ray analyses also suggest that free rotation is allowable for $\omega_5$, whereas $\omega_4$ is constrained to the *trans*-conformation. This tendency is ascertained by the energy contour map of ($\omega_4$, $\omega_5$) shown in Fig. 3b. It can be seen from Fig. 3c that there are several minima for the rotational energy of $\omega_5$ and $\omega_6$, as indicated on the contour map. However, the $\omega_5$ and $\omega_6$ region, close to (±90°, ±90°), is more stable than that of $\omega_5$ = 180° by 1–2 kcal/mol.

The stable torsion angles estimated from the theoretical conformational energy analyses are, on the whole, in good agreement with those observed in the X-ray analyses, suggesting that the molecular conformations revealed by X-ray analyses (Fig. 1) represent the inherent stable forms for the respec-

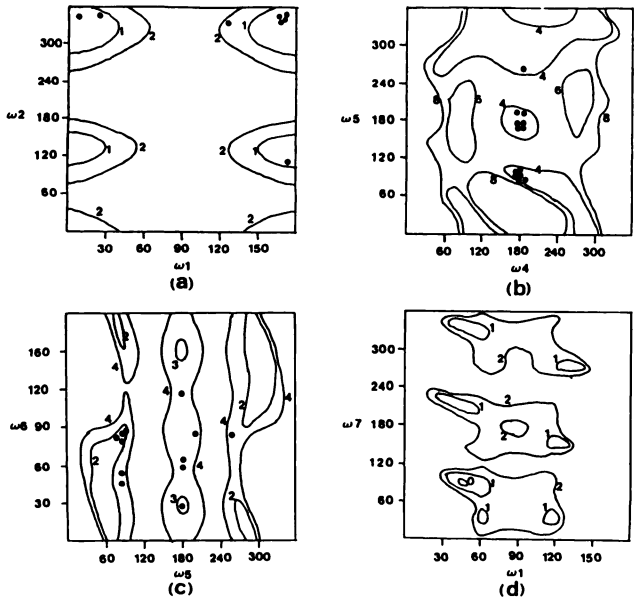


**Fig. 3.** Contour energy maps of ($\omega_1$, $\omega_2$) (a), ($\omega_4$, $\omega_5$) (b), ($\omega_5$, $\omega_6$) (c), and ($\omega_1$, $\omega_7$) (d). The *number* in the map represents the relative energy value (kcal/mol).

tive compounds and can be used for the analyses of quantitative structure—activity relationships. Encouraged by these results, the most possible conformation of compound **4** proposed is shown in Fig. 4. This conformation is essentially the same as compounds **1a**, **2**, and **3**, except for $\omega_1$. When **4** takes a conformation at $\omega_1$ of 180°, the strict steric hindrance occurs between the phenyl ring and the *tert*-butyl group, clearly seen in Fig. 3d). In contrast, the conformation at $\omega_1$ of 90° is in the global minimum, allowing rotational freedom for the torsions $\omega_1$ and $\omega_7$ (atoms 3–4–41–42). The most stable conformation is at $\omega_1$ of 45° and $\omega_7$ of 90°, as shown in Fig 4.

### Structure-Activity Relationships

For the purpose of geometric analysis for the inhibitory activity, it is important to consider which groups participate in the binding to aldose reductase. Although the absence of detailed structural information on the enzyme frustrates this consideration at present, the following discussion on the structural and conformational comparisons with the inhibitory activity leads to the conclusion that the benzyl 5-phenyl-2-oxazolecarbamate skeleton and its spatial conformation are absolutely necessary for the emergence of activity.

The replacement of the 5-phenyl ring (**1–5**) with the methyl (**7** and **9**) or *tert*-butyl groups (**6**) causes drastic decrease in the inhibitory activity, implying the importance of the hydrophobic aromatic ring at the oxazole C5-site and its coplanar formation with the oxazole ring (compare **1–3** with **4**). As exemplified by the compounds **10** through **12**, the structural modification of the oxazole ring itself (**12**) or the binding site of the phenyl and carbamate chains (**10** and **11**) also causes drastic three-dimensional changes (see Fig. 1), consequently leading to complete inactivation. On the other hand, the existence of the benzyl end-group and its spatial orientation with respect to the oxazole ring are also important for activation (compare compounds **1–3** with **5** and **8**). It is conceivable from these facts that the binding site of aldose reductase for 2-oxazolecarbamate compounds has a well defined spatial orientation (binding specificity) and that the hydrophobic interactions between the phenyl and the benzyl rings, as well as the hydrogen bonds in which the N and/or O atoms of oxazole ring and amide group participate, are essential for the best binding with the receptor.

It is of special importance to note that the highly active benzyl 5-phenyl-2-oxazolecarbamates (**1–3**) all show the following conformational similarities, irrespective of the substituents at the oxazole C4-site: $\omega_1 = \sim 180°$, $\omega_2 = \sim 0°$, $\omega_3 = \omega_4 = \sim 180°$, $\omega_5 = \sim 90°$, and $\omega_6 = \sim -90°$. This conformation is also energetically stable, as seen from Fig. 3. Therefore, it is reasonable to conceive that **1–3** represent the best-fit forms for the binding pocket of the reductase (the surface contour mapping for **1a** is shown in Fig. 5). In addition to the conformational similarities, compounds **1–3** show similar characteristics in their dipole moments; their dimensions and directions with respect to the oxazole ring fixed at the orientation shown in Fig. 1 are in the narrow range of 1.2–1.5 D for the $x$ (horizontal, $\mu_x$), −0.3–0.1 D for the $y$ (vertical, $\mu_y$), and 1.3–1.7 D for the $z$ direction (perpendicular to $x$ and $y$, $\mu_z$). The other compounds (**4–12**) exhibited dipole moments more or less deviated from this range. On the other hand, the inhibitory activity of benzyl 5-phenyl-2-oxazolecarbamate analogues (**1–5**) appears to be related to the bulkiness of the alkyl group attached at the oxazole C4-site, in addition to the molecular conformations; the activity increases in the order of —H (**5**) < —$C(CH_3)_3$ (**4**) < —$CH_3$ (**3**) < —$CH_2CH_3$ (**2**) < —$CH(CH_3)_2$ (**1**) (their Taft steric substituent constants (25) are −1.12, 1.43, 0.0, 0.08, and 0.48, respectively). A reason for compound **4** having less activity than **1** is due to the deviation of the 2-phenyl ring from the coplanar formation with the oxazole ring.

In order to clarify the relationship between the above-mentioned chemical and conformational characteristics and their activities, a QSAR analysis was carried out in which compounds **1–9** were considered. The results are given in Table 6. The contribution of log $P$ (lipophilicity) to the activity is relatively poor when all compounds are taken into account (compare Eq.

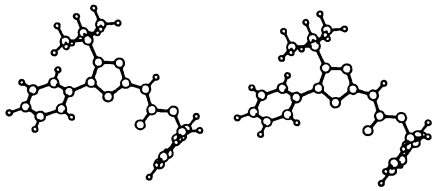

**Fig. 4.** Most probable molecular conformation of compound **4** proposed from theoretical energy calculations.

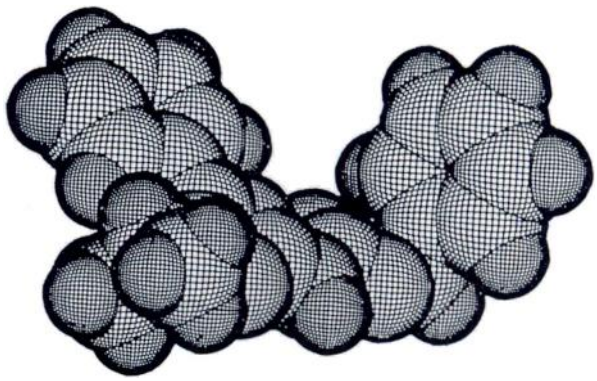

**Fig. 5.** Surface-contoured molecular conformation of compound **1a**.

TABLE 6
**Correlation coefficients of QSAR parameters and correlation equations for inhibitory activities**

| | log *P* | $E_s^{4a}$ | $E_s^{5b}$ | $\mu_x$ | $\mu_y$ | $\mu_z$ | MSA | CDV |
|---|---|---|---|---|---|---|---|---|
| Linear correlation coefficients used for QSAR analyses | | | | | | | | |
| $r^c$ | 0.516 | 0.512 | 0.684 | 0.489 | 0.326 | 0.842 | 0.696 | 0.913 |
| | | | | | | $n^d$ | *r* | SD[e] |
| Correlation equations for inhibitory activities | | | | | | | | |
| Eq. 1: $\log(1/IC_{50}) = -0.0417 - 0.0327$ CDV | | | | | | | | |
| | (0.2352) (0.0046) | | | | | 11 | 0.913 | 0.457 |
| Eq. 2: $\log(1/IC_{50}) = -0.0424 + 0.0022 \log P - 0.0326$ CDV | | | | | | | | |
| | (0.2424) (0.1801) (0.0056) | | | | | 11 | 0.913 | 0.457 |
| Eq. 3: $\log(1/IC_{50}) = -0.9091 + 0.0024$ MSA $- 0.0303$ CDV | | | | | | | | |
| | (1.7530) (0.0048) (0.0065) | | | | | 11 | 0.915 | 0.451 |
| Eq. 4: $\log(1/IC_{50}) = -0.2808 - 0.3903\ \mu_z - 0.0226$ CDV | | | | | | | | |
| | (0.1590) (0.0988) (0.0038) | | | | | 11 | 0.967 | 0.286 |
| Eq. 5: $\log(1/IC_{50}) = -0.7196 + 0.2767\ E_s^5 - 0.0279$ CDV | | | | | | | | |
| | (0.4739) (0.1734) (0.0051) | | | | | 11 | 0.931 | 0.408 |
| Eq. 6: $\log(1/IC_{50}) = -0.3324 + 0.2237\ E_s^5 - 0.3799\ \mu_z - 0.0225$ CDV | | | | | | | | |
| | (0.3022) 0.1443) (0.1174) (0.0039) | | | | | 11 | 0.976 | 0.243 |

[a] Taft's steric substituent constant at oxazole C4-site.
[b] Taft's steric substituent constant at oxazole C5-site.
[c] Correlation coefficient with inhibitory activity.
[d] Number of data used in regression.
[e] Standard deviation from regression line.

1 with Eq. 2). A good correlation is obtained with the CDV (Eq. 1) rather than with the MSA (Eq. 3), implying that the inhibitory activity is largely dependent on the molecular conformation. This conformational importance for the activity emergence can also be suggested from the correlation with the dipole orientation of the *z* direction ($\mu_z$) (Eq. 4). Furthermore, the existence of the phenyl ring at the oxazole C5-site is also important for the effective activity emergence (see Eqs. 5 and 6).

The present results derived from the combination of X-ray crystallographic and QSAR analyses clearly showed that the molecular conformation is very important for the inhibitory activity of oxazole compound. Therefore, it is very interesting to consider how this insight relates to the understanding of another potent aldose reductase inhibitor. Kador *et al.* (16, 26) have proposed a possible interaction mode between aldose reductase and its inhibitor, based on the electrostatic and steric features of various inhibitors. According to this model, the binding pocket of the enzyme consists of two hydrophobic (H1 and H2) and a charge-transfer (CT) site, and the relative disposition among these three sites is very important for the tight binding with the inhibitor. The CT site, which is located adjacent to the two hydrophobic binding sites, is responsible for the hydrogen bonding with the polar atoms within the inhibitor. It is interesting to see that the conformational significance concluded from the present study can be well supported by this binding model. Judging from the comparison of the molecular conformation shown in Fig. 5 with the schematic diagram of the binding model (see Fig. 3 of Ref. 16), the coplanar 5-phenyloxazole moiety (A), terminal benzyl group (B), and the carbamate group (C) appear to bind well with the H1, H2, and CT sites of the enzyme, respectively. The distances of A(center)–B(center), A(center)–CT(C22), and CT(C22)–B(center) are 7.88, 3.12, and 4.30 Å, respectively, and are in the region proposed for other potent inhibitors. Furthermore, the present molecular shape analyses have proposed that the H1 site is at almost right angles to the H2 one (the averaged dihedral angle between A and B planes is 103.3° for **1**–**3**).

Drug design of more potent analogues is now in progress, based on the present insights.

**References**


1. Varma, S. D., and J. H. Kinoshita. Sorbitol pathway in diabetic and galactosemic rat lens. *Biochim. Biophys. Acta* **338**:632–640 (1974).
2. Jedziniak, J. A., L. T. Chylack, Jr., H. M., Cheng, K. Gillis, A. A. Kalustian, and W. H. Tung. The sorbitol pathway in the lens: aldose reductase and polyol dehydrogenase. *Invest. Ophtalmol. Visual. Sci.* **20**:314–326 (1981).
3. Gabbay, K. H., L. O. Merola, and R. A. Field. Sorbitol pathway: presence in nerve and cord with substrate accumulation in diabetes. *Science* (*Wash. D. C.*) **151**:209–210 (1966).
4. Ward, J. D. Polyol pathway in the neuropathy of early diabetes. *Adv. Metab. Disord. Suppl.* **2**:425–429 (1973).
5. Heath, H., and Y. C. Hamlett. The sorbitol pathway: effect of streptozotocin induced diabetes and the feeding of a sucrose-rich diet on glucose, sorbitol and fructose in the retina, blood and liver of rats. *Diabetologia*, **12**:43–46 (1976).
6. Corder, C. N., J. G. Collins, T. S. Brannan, and J. Sharma. Aldose reductase and sorbitol dehydrogenase distribution in rat kidney. *J. Histochem. Cytochem.* **25**:1–8 (1977).
7. Kinoshita, J. H. Mechanisms initiating cataract formation. *Invest. Ophthalmol.* **13**:713–724 (1974):
8. Kinoshita, J. H., P. Kador, and M. Catiles. Aldose reductase in diabetic cataracts. *J. Am. Med. Assoc.* **246**:257–261 (1981).
9. Beyer, T. A., and N. J. Hutson. Evidence for the role of the polyol pathway in the pathophysiology of diabetic complications. *Metab. Clin. Exp.* **35**:1–3 (1986).
10. Kador, P. F., Y. Akagi, and J. H. Kinoshita. The effect of aldose reductase and its inhibition on sugar cataract formation. *Metab. Clin. Exp.* **35**:20–23 (1986).
11. Sarges, R., J. Bordner, B. W. Dominy, M. J. Peterson, and E. B. Whipple. Synthesis, absolute configuration, and conformation of the aldose reductase inhibitor sorbinil. *J. Med. Chem.* **28**:1716–1720 (1985).
12. Kakuta, H., N. Hotta, M. Kimura, H. Fukasawa, N. Koh, N. Sakamoto, and M. Iida. In *Current Topics in Clinical and Experimental Aspects of Diabetes Mellitus* (N. Sakamoto, H. K. Min, and S. Baba, eds.). Excerpta Medica, Amsterdam, 376 (1984).
13. Robison, W. G., Jr., P. F. Kador, Y. Akagi, J. H. Kinoshita, R. Gonzalez, and D. Dvornik. Prevention of basement membrane thickening in retinal capillaries by a novel inhibition of aldose reductase, tolrestat. *Diabetes* **35**:295–299 (1986).
14. Tanimoto, T., H. Fukuda, T. Yamaha, Y. Ohmomo, M. Nakao, and C. Tanaka. Inhibitory effect of benzyl oxazolecarbamate analogues on aldose reductase. *Chem. Pharm. Bull.* (*Tokyo*) **34**:2501–2505 (1986).
15. Tanimoto, T., H. Fukuda, J. Kawamura, M. Nakao, U. Shimada, A. Yamada, and C. Tanaka. Inhibition of aldose reductases from rabbit lens by oxazole derivatives. *Chem. Pharm. Bull.* (*Tokyo*) **32**:1032–1039 (1984).
16. Kador, P. K., J. H. Kinoshita, and N. E. Sharpless. Aldose reductase inhibi-

tors: a potential new class of agents for the pharmacological control of certain diabetic complications. *J. Med. Chem.* **28**:841–849 (1985).
17. Main, P., G. Germain, and M. M. Woolfson. MULTAN84, a computer program for the automatic solution of crystal structures from X-ray diffraction data. University of York, England (1984).
18. Ashida, T. The Universal Crystallographic Computing System-Osaka, UNICS-Osaka. The Computer Center, Osaka University, Osaka, Japan (1979).
19. Cromer, D. T., and J. T. Waber. In *International Tables for X-Ray Crystallography* (J. A. Ibers, and W. C. Hamilton, eds.), Vol. 4. Kynoch Press, Birmingham, 71 (1974).
20. Molecular Design, Ltd., CHEMLAB-II, a molecular modeling software system. San Leandro, CA (1986).
21. Pople, J. A., and G. A. Segal. Approximate self-consistent molecular orbital theory. III. CNDO results for $AB_2$ and $AB_3$ system. *J. Chem. Phys.* **44**:3289–3296 (1966).
22. Hopfinger, A. J., and R. A. Pearlstein. Molecular mechanics force-field parameterization procedures. *J. Comput. Chem.* **5**:486–499 (1984).
23. Hopfinger, A. J. A QSAR investigation of dihydrofolate reductase inhibition by baker triazines based upon molecular shape analysis. *J. Am. Chem. Soc.* **102**:7196–7206 (1980).
24. Pearlstein, R. A. Ph.D. dissertation, Case Western Reserve University, Cleveland, OH (1983).
25. Macphee, J. A., A. Panaye, and J. E. Dubois. Steric effects. I. A critical examination of the taft steric parameter -Es: definition of a revised, broader and homogeneous scale: extension to highly congested alkyl groups. *Tetrahedron* **34**:3553–3562 (1978).
26. Kador, P. F., and N. E. Sharpless. Pharmacophor requirements of the aldose reductase inhibitor site. *Mol. Pharmacol.* **24**:521–531 (1983).

**Send reprint requests to:** Dr. Toshimasa Ishida, Division of Physical Chemistry, Osaka University of Pharmaceutical Sciences, 2-10-65 Kawai, Matsubara-City, Osaka 580, Japan.